On the Dynamics of Globular Clusters in Eccentric Orbits

by

Karin Roley

Bachelor of Arts – Department of Astrophysical & Planetary Sciences

Undergraduate Honors Thesis

Defense Copy

Thesis Defense Committee:

Prof. Ann-Marie Madigan	Advisor/Honors Council Representative	Department of APS
Prof. Andrew Hamilton	External Faculty Member	Department of APS
Prof. Katharine Semsar	External Faculty Member	Miramontes Arts and Sciences Program

To defend on:

March 31, 2022

This thesis entitled:
On the Dynamics of Globular Clusters in Eccentric Orbits
written by Karin Roley
has been approved for the Department of Astronomy

Prof Prof. Ann-Marie Madigan

Prof. Andrew Hamilton

Prof. Katharine Semsar

Date

The final copy of this thesis has been examined by the signatories, and we find that both the content and the form meet acceptable presentation standards of scholarly work in the above mentioned discipline.

Roley, Karin (B.A., Astronomy)

On the Dynamics of Globular Clusters in Eccentric Orbits

Thesis directed by Prof Prof. Ann-Marie Madigan and Dr.Maria Tiongco

The dynamics of globular clusters in circular orbits have been studied in the past, but their dynamics in eccentric orbits are still unclear. Most globular clusters are in an eccentric orbits around their host galaxy, thus learning about their dynamics in such orbits will lead to a better understanding of their nature. For this reason, we explore the long term effect of eccentric orbits of globular clusters around their host galaxy using NBODY6, an N-body simulation package specializing in star clusters. Specifically, we look at the effect of eccentric orbits on the mass loss rate of globular clusters, orientation of the angular momentum vector($\mathbf{L}$) and angular velocity vector(ω) of the clusters in both Cartesian and spherical coordinates, and study the behaviours of these vectors in three equal mass sections inside the cluster. We find similar results as past research: the angular momentum and angular velocity decreases due to the cluster's mass loss from dynamical friction. We also found that for cluster with eccentric orbits, the angular momentum vector of a cluster evolves in a step function with its period corresponding to the orbital period of the cluster. The angular velocity on the other hand has rapid increases at the pericenter and decreases while approaching apocenter. When looking at the evolution in spherical coordinates, defining the direction of angular momentum away from the z-axis to be L_θ and the direction of angular momentum away from the x-axis to be denoted as L_ϕ, we find that while L_{phi}'s evolution is dependent on the orbital period of the cluster, L_θ is dependent on the mass remaining. Finally, when we split the cluster into 3 equal mass section, the angular momentum of the outer radius is larger than the other regions, while angular velocity is the largest in the inner region when calculated in the Cartesian coordinates. In spherical coordinates, L_ϕ does not vary between the 3 sections, and L_θ is strongest in the inner regions, followed by the middle region and with the outer regions having the weakest magnitude.

Dedication

To my family: Takako, Donald, and Kenji Roley.

Acknowledgements

I would like to thank Maria Tiongco for her mentor-ship and time as well as Ann-Marie Madigan for guiding me through the process, as I would not have been able to come this far without them. I would also like to thank Ann-Marie's research group for their support and advice. I would also like to thank Andrew Hamilton and Katherine Semsar for being a part of my honors committee and their advise. Finally, I would like to thank JILA and RMACC for letting me borrow their equipment and generally helping me through the process.

Contents

Tables

Table

Figures

Figure

Chapter 1

Introduction

A Globular cluster is class of star clusters mostly spherical in shape with a high density of stars at its core due to the strong gravitational interaction between each stars. They are often found in the halo region of galaxies, and consists of some of the oldest stars in the universe. Figure 1.1 shows an example of such a star cluster. Due to these conditions, globular clusters have been a subject of study for many astrophysicists, as they shed light to varying topics in the field, such as origins of old stars, possible existence of intermediate mass black holes, and the creation of galaxies.

One example of such study is Bar et al. (2022), an observational study analyzing the data of the galaxy NGC5846-UDG1, which contains a large amount of globular clusters. They use the presence of globular clusters in order to calculate the dynamical friction present in the galaxy.

As demonstrated above, there are various studies done using globular clusters, thus it is important to learn the foundation of such systems to expand the filed of astrophysics. Yet, theoretical studies concerning their angular momentum and angular velocities are scarce. There are multiple reasons for this, one of which comes from the fact that the image of rotating globular clusters is a newer revelation that resulted from better observational data(see Fabricius et al. (2014)). Due to the increasing number of evidence of rotating globular clusters, studies concerning the role of angular momentum in cluster evolution have been gaining more attention.

Thus, it is important to study globular clusters and their rotation, in both theoretical and observational study, in order to advance the knowledge in the field of astrophysics. One example of this being done on the theoretical side is Tiongco et al. (2018). The study found that when

Figure 1.1: Hubble image of Messier 80, a globular cluster located 30,000 light-years away from Earth. https://esahubble.org/images/opo9926a/

a cluster is on a circular orbits around its host galaxy, it slowly loses mass due to the dynamical friction between individual stars, a process in which the gravitational interactions between stars cause the heavier mass to sink towards the center and lighter mass to be ejected from the system. This leads to a decrease in angular momentum/velocity of the globular cluster as it evolves with time. This study shed light into the nature of a rotating globular cluster, however, it is not enough to describe many globular clusters found in our universe.

The reason for this is the scarcity of globular clusters in circular orbits. According to Ninkovic (1983), almost all globular clusters found in our universe are in an eccentric orbits, with most cluster's eccentricity ranging from 0.3-0.65. In order to apply the theoretical calculations to observational studies, we must expand the result of previous theoretical studies to include the effect of eccentric orbits.

It has also been suggested that mass plays a large role in the evolution of a globular cluster's internal kinematics. Webb et al. (2014), an N-body study on the evolution of half mass relaxation time(which is the time it takes for stars to lose information on their initial conditions) and velocity dispersion of globular clusters, shows that mass loss rate has a large effect on the evolution of a cluster's velocity dispersion.

The goal of this paper is to determine how much of the results in Tiongco et al. (2018) can be applied to eccentric orbit simulations, and if results in Webb et al. (2014) can be extended to angular momentum and angular velocity. To do this we study how the internal kinematics of globular clusters are effected by eccentric orbits around its host galaxy using NBODY6: an N-body simulation system that are often used to simulate systems like globular clusters. Specifically, we will look at the angular momentum vector($\mathbf{L}$) and angular velocity vector(ω) and their time evolution in both Cartesian and spherical coordinates. We will also look at the variation in these two vectors in three equal mass section within the globular cluster, to verify past results and expand on the internal kinematics of globular clusters.

Chapter 2

Methods and Initial Conditions

2.1 Methods

An N-body problem in astrophysics refers to the method of calculating the interactions between particles caused by their gravity. This is very difficult to do by hand, due to the fact that in most cases the number of particles in the system, denoted by N, is extremely large. An accurate N-body problem would require us to calculate the interactions of each particles with every other particles in the system. Thus a computer simulation is necessary, especially for systems like globular clusters, where N is on the scale of 10^5 at minimum.

A popular simulation package used for globular clusters is the simulation program NBODY6. It calculates the position and velocity of each particles by using direct integration method of Newtonian mechanics, calculated at a specific time steps. There are limitations to such a program, specifically the fact that efficiency and accuracy must be at a balance in such a software. Realistically, we would like to consider a system with as many particles as we need to gain a full understanding of realistic star clusters, however, putting too many particles will put a constraint on the computer. Thus, we must consider enough particles in the system to gain an accurate result, while putting in the least amount of particles as possible to maximize the efficiency of the simulation.

Simulations of various globular clusters were completed on NBODY6, which we used afterwards to find the angular velocity and momentum of the cluster. This was done by taking the mass, position, and velocity of individual stars and calculating their angular momentum in both

Cartesian and spherical coordinates. We summed individual angular momentum and angular velocity calculated in order to find the total for the cluster. We split up the cluster to three equal mass section based on the third mass radius: radius in which where the 3rd of the total mass of the cluster is contained in. We then calculated the angular momentum and velocity for each section, similarly to when calculating the total, to obtain the angular momentum and velocity of each section.

2.2 List of Initial Conditions

In order to maximize the efficiency of the simulations while keeping its accuracy, we implemented several limitations. First, the host galaxy is assumed to be a point mass which the cluster orbits starting from apocenter, and in a fixed orbit throughout the simulation. We assumed the cluster to be a local system where effects of dark matter is negligible, and thus was not considered in this study. The clusters started with 32,768 equal mass stars in the system, and note that dynamical friction is still relevant, as the gravitational interactions between the particles are enough to cause the mass loss and more importantly, core collapse: a process in which a globular cluster collect high density of stars towards their cores that it creates a defined cusp of light. Although there is no initial ϕ angle, ω_θ and L_ϕ both have an initial tilt of 45 degrees, as that was the angle found to have the most notable effect on the cluster by Tiongco et al. (2018).

The set up for the simulations were as follows: the orbital plane of the cluster is defined as the x-y plane in Cartesian coordinates, with the z-axis perpendicular to the plane. The location of the host galaxy is defined as the origin with the apocenter in the positive x-axis, while the pericenter resides in the negative x-axis. ϕ describes the anti-clockwise angle in the orbital plane, while θ describes the angle measured from the z-axis. A schematic representation of this set up is represented in figure 2.1. Spherical components of angular momentum will be denoted with L_θ and L_ϕ respectively, and the spherical components of angular velocity will be denoted by ω_θ and ω_ϕ. Similarly, the Cartesian components of angular momentum will be represented with L_x, L_y, and L_z, and Cartesian components of angular velocity will be denoted as ω_x, ω_y, and ω_z. Due to how

the simulations were set up for circular orbits and eccentric orbits, the circular orbit simulations were solved using rotating reference frame, and the eccentric orbits were solved with a non-rotating reference frame.

Simulations for this study were run by NBODY6 (see Nitadori and Aarseth (2012b)), accelerated by a graphic processing unit(see Nitadori and Aarseth (2012a)) on the RMACC Summit Super Computer at the University of Colorado Boulder. The scales of the gravitational constant and the initial mass of the clusters are set as G=M=1, and initial energy as E=-0.25 by code unit (see Heggie and Hut (2003)). Thus, all results presented in this paper will be normalized to some constant for the purpose of generalization. The initial conditions were sampled from the distribution function (which gives the initial positions and velocities of individual stars) from Varri and Bertin (2010), which generates rotating star clusters that flatten it into an oblate structure along rotation axis.

The initial half mass relaxation time, defined as the time it takes for a system of particles to forget its initial conditions are defined by the following equation:

$$t_{rh,i} = \frac{0.138 N^{1/2} r_h^{3/2}}{< m >^{1/2} G^{1/2} log(0.11)} \tag{2.1}$$

Where N denotes the initial number of particles inside a cluster, $r_{\rm h}$ denotes the initial half mass radius of the cluster, M denotes the initial mass, and G is the gravitational constant. As all cluster start with the same physical characteristics, $t_{\rm rh,i} = 414.5587$ will be the same for all of them, time evolution of each simulations will be normalized to this constant.

A total of 6 simulations were done for this study, 4 of which are in eccentric orbits. List of all simulations can be found in table 2.1. The two circular orbits are of varying distances from its host galaxy, decided by the percentage that fills the Jacobi radius $r_{\rm J}$: an approximation for the size of the tidal boundary (where the gravitational potential of the star cluster dominates over the potential of the galaxy), and also defined as the following:

Figure 2.1: Schematic representation of the simulation set up.

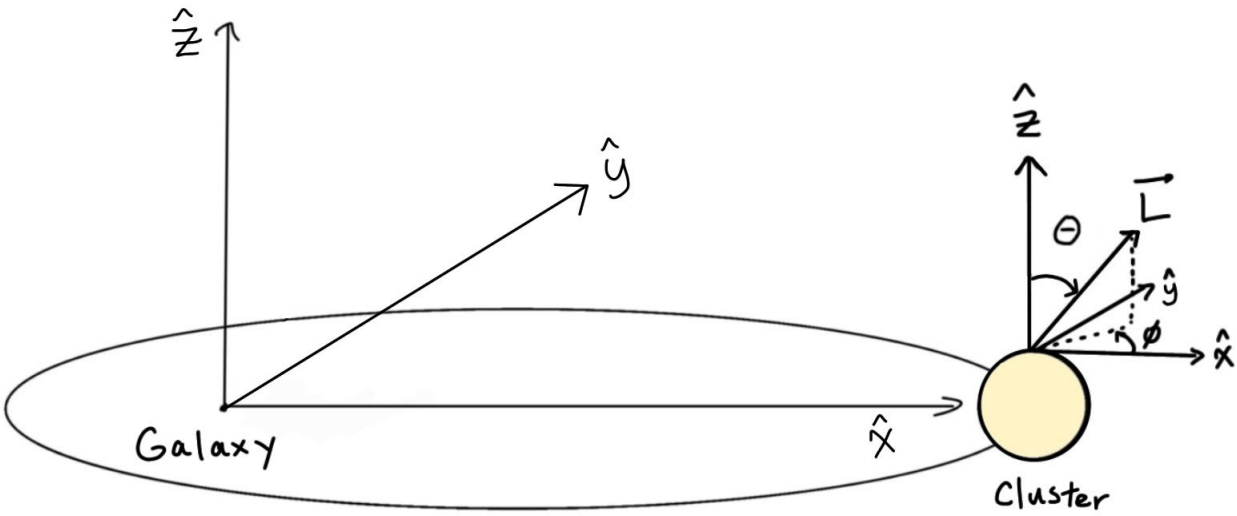

$$r_J = (\frac{G}{3\Omega^2})^{\frac{1}{3}} M^{\frac{1}{3}} \tag{2.2}$$

If the radius of a star's orbit measured from the core of the cluster is larger than r_J, it was considered to have been lost from the cluster, and thus were not considered when calculating for **L** and ω. The more the cluster's radius fills the Jacobi radius, the closer they are to their host galaxy, thus more likely for the cluster to lose their mass. As naming convention, F075 fills 75% of the Jacobi radius, while F025 fills 25% of the Jacobi radius. Thus, F025 is the cluster that is further away from the host galaxy.

Table 2.1: Table showing the list of simulations. e denotes the eccentricities of each simulations. Out of the 6 simulations, 2 have circular orbits and 4 have eccentric orbits.

Model ID	e
F075	0
F025	0
E02	0.2
E04	0.4
E06	0.6
E08	0.8

The distance of the eccentric orbits simulation from their host galaxy depended on the eccentricity of the cluster's orbit. The pericenter of all eccentric orbit simulations were the same distance as the orbit of F075, and the distance of the apocenter was adjusted accordingly to give its orbit the desired eccentricities. Thus, caution is needed when analyzing the results obtained to distinguish the effects of distance versus eccentricity. The distance of apocenter and pericenter of the cluster normalized to the distance of F075 is presented in table 2.2.

The simulations were run until at least 15 $t_{\rm rh,i}$, and when possible, until only 25% of the mass were remaining. The disparity in simulation times were caused by core collapse. Once a globular cluster undergoes core collapse, the simulations become too difficult to continue due to the small distances between individual particles.

Table 2.2: This table shows the distance of the cluster from its host galaxy at pericenter and apocenter, normalized to the distance of F075 cluster. With the exception of F025, which stays at the further radius from F075 at all time, all simulations have the same pericenter, with the apocenter increasing with eccentricity.

Model ID	Pericenter	Apocenter
F075	1	1
F025	3	3
E02	1	1.55
E04	1	2.58
E06	1	5.19
E08	1	15

Chapter 3

Results

3.1 Mass Loss Rate of Each Cluster

Before analyzing $\mathbf{L}$ and ω, it is important to understand the mass loss rate of each simulations. This is due to the fact that $\mathbf{L}$ is proportional to the mass of the cluster. Thus this section will provide a short description of how mass loss rate differs between each simulations.

Figure 3.1 shows the time evolution normalized to the mass remaining in the globular cluster for each simulation, where time t is normalized to $t_{\rm rh,i}$ and the instantaneous mass m is normalized to the initial mass of the system M. As previously mentioned, only a few simulations avoided complications due to core collapse and continued until 25% of the mass were remaining. Thus higher eccentric orbits like E06 and E08 kept large amount of their initial mass as the end of the simulation. As expected, the overall trend of the cluster's mass loss is that it decreases with time due to the dynamical friction ejecting mass out of the system.

The distance of the cluster from the host galaxy also affects the mass loss rate, as can be seen in the figure for F075(top left) and F025(top middle). While F075 reaches the remaining mass of 25% at 14 t/$t_{\rm rh,i}$, F025 reaches the same point at 60 t/$t_{\rm rh,i}$. In Tiongco et al. (2018), it was predicted that systems with larger distance from the host galaxy evolves slower than those that are closer due to the reduced tidal force from the galaxy. When the cluster is close to the galaxy, the individual stars will feel a stronger gravitational force from the host galaxy, and makes it easier for them to escape the cluster. Thus, F025 losing mass at a slower rate compared to F075 is supported by previous studies and predictions.

For simulations F075, E02, and E04, a slight bent in the mass loss can be seen, causing the mass loss rate speed up slightly. This is likely due to the effect of core collapse. Once core collapse occurs, the density of the inner region increases while the density of out region decreases. It is thus easier for the outer stars to be pulled away from the cluster, speeding up the mass loss rate.

More interesting effects can be seen in the higher eccentric orbits as E04, E06 and E08, where the mass loss rate is a step function corresponding to their orbital period. Due to their eccentric orbits and larger distance from the host galaxy, high eccentric orbits tend to spend most of their lifetime near its apocenter where it loses mass at a slower rate than when they are in pericenter. The cluster loses less mass when it is in apocenter compared to when in pericenter, thus leading to the step function like results we see in figure 3.1.

Figure 3.1: This figure shows the time evolution t normalized to $t_{\mathrm{rh,i}}$ of the mass m remaining in the system normalized to the initial mass M.

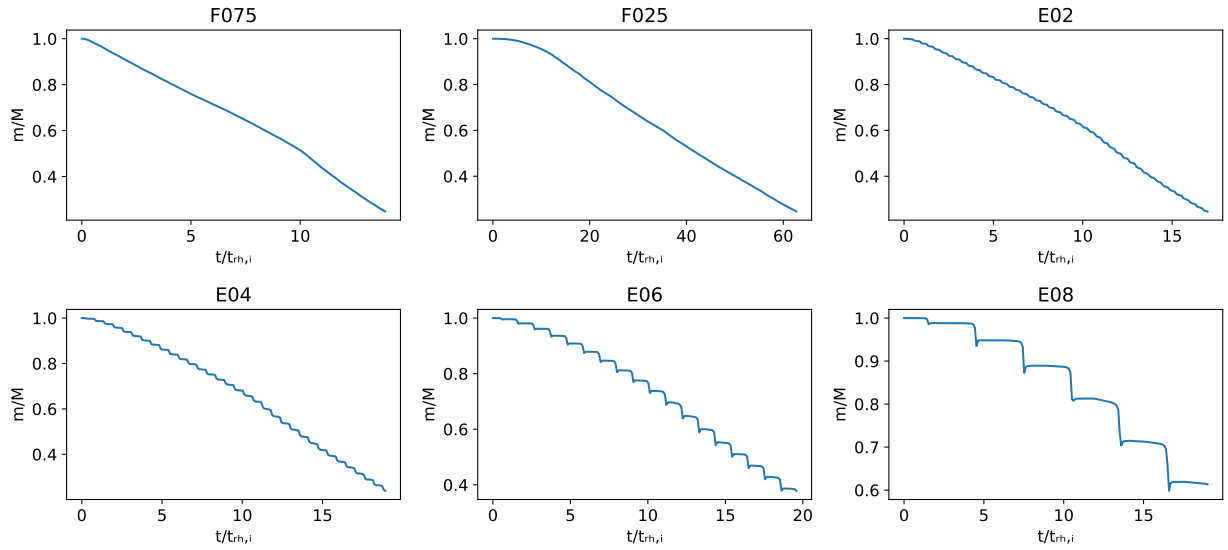

For the rest of the paper, we will use the mass loss of each simulation in order to infer what kinds of effects a cluster's orbit has on the evolution of $\mathbf{L}$ and ω. In the next section we will calculate the Cartesian components of these two vectors.

3.2 Evolution of Angular Momentum and Velocity in Cartesian Coordinates

Figure 3.2: This figure shows the time evolution t normalized to $t_{\mathrm{rh,i}}$ of angular momentum L in varying Cartesian coordinates. The red line shows the magnitude of **L**, while the x, y, z components of the vector are represented by the blue, yellow, green lines respectively. The magnitude shows a step-function like behaviour for higher eccentric orbit.

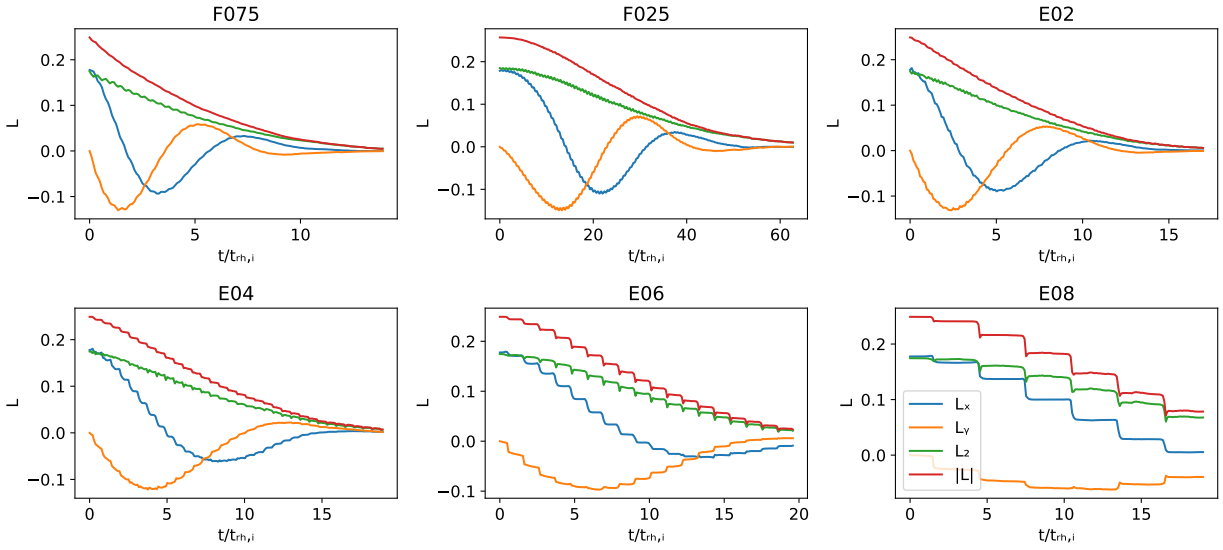

Angular velocity, and mass of a system affects the angular momentum of the cluster as it evolves with time. Thus, it is important to study and compare them carefully in order to gain a better understanding of the cluster's evolution. First, we will look at time evolution of **L** for each cluster. Figure 3.2 plots the time evolution of **L** in Cartesian coordinates, where time is normalized to $t_{\mathrm{rh,i}}$.

The step function like behaviour seen in high eccentric orbits of figure 3.1 is also present in figure 3.2. For eccentric orbits like E04, E06, and E08, the step function can be seen in all components of x,y, and z, suggesting that mass loss is proportional the evolution of angular momentum. Note that the step function like behaviour also exists in E02, but are not as visible as the other eccentric orbit clusters as the orbital period of E02 is too quick to make a notable step function.

There are various trends that can be seen across all simulations, namely the sinusoidal evolution in L_x and L_y component of the vector. In all simulations, L_y starts at 0 and decreases,

while L_x starts at non-zero and decreases. The sinusoidal evolution in x and y suggests a precession of angular momentum shown by figure 3.3, which plots L_x and L_y together in order to show the precession in more detail. Although there are some fluctuations corresponding to the orbital motion, overall the angular momentum vector spirals inwards as it evolves with time, with stronger precession for circular and lower eccentric orbits compared to the higher ones. This effect was found in the circular orbit simulation from Tiongco et al. (2018). Thus, so far our results align with those that were suggested in previous studies. One thing to note about the precession, is that as the eccentricity of the orbits increase, the less the precession becomes notable. This likely comes from the fact that high eccentric orbits spent most of their times at apocenter, where they did not feel the tidal force as much as the more circular orbits did, leading to the weaker precession.

Figure 3.3: A top down view of the evolution of **L** as seen from the z-axis. The path followed by the **L** vector in the x-y plane is shown for each simulation. The simulations start with the outer end of the spiral while moving inwards as the cluster evolves with time.

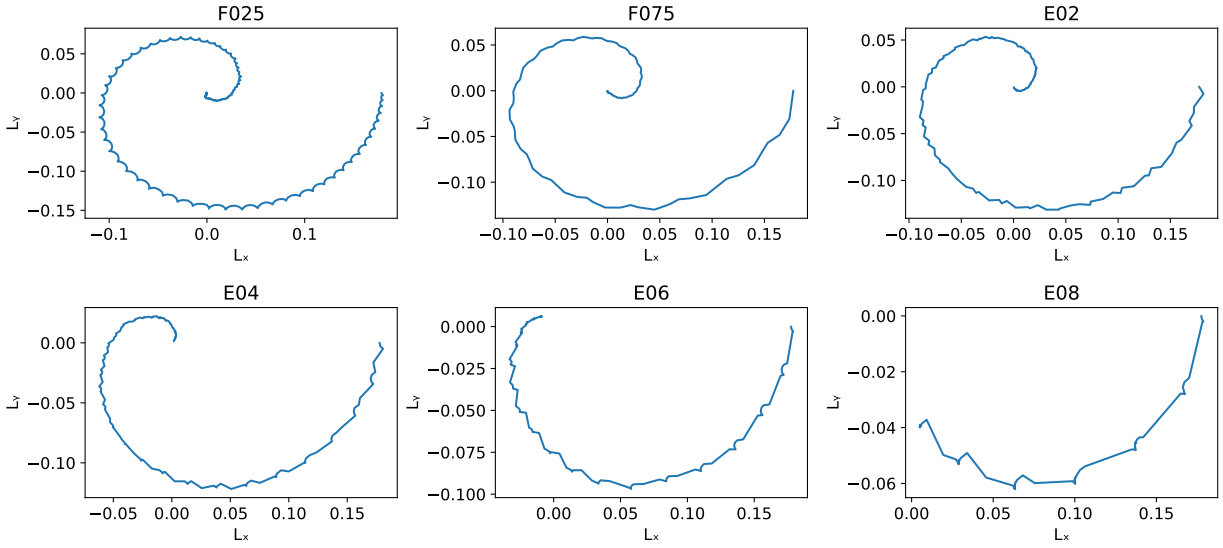

Figure 3.4 plots the time evolution of angular velocity vector ω in Cartesian coordinates for all simulation. In each plot, ω is normalized by the angular velocity at pericenter: Ω_p. As usual, time t is normalized to $t_{\mathrm{rh,i}}$. Similarly to the angular momentum, the angular velocity of the system generally decreases as it evolves with time, with all components eventually approaching

Figure 3.4: This figure shows the time evolution t normalized to $t_{\mathrm{rh,i}}$ of angular velocity ω in varying Cartesian coordinates. ω is normalized by the angular velocity at pericenter of the cluster's orbit Ω. The red line shows the magnitude of ω, while the x, y, z components of the vector are represented by the blue, yellow, green lines respectively. Although similar to **L** plot, the main distinction is the periodic increase of the graph rather than the step function.

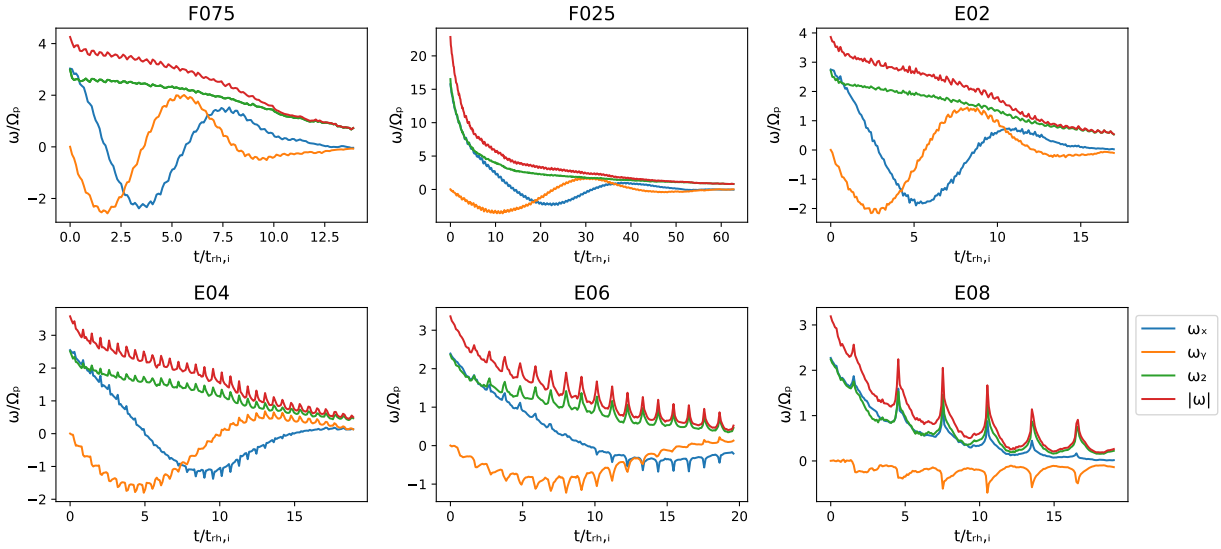

zero. However, the step function like behaviour seen in mass and **L** is not present in ω.

Instead, ω of high eccentric orbits shows a nutation(periodic peaks) corresponding to the orbital period of the cluster. This result was seen in the study done by Webb et al. (2014) which was explained as gravitational potential energy being converted to kinetic energy when it approaches the host galaxy, leading to a momentary increase in ω. The main difference between our study and Webb et al. (2014) is that Webb et al.'s simulation contained thermal energy, while ours did not.

The varying behaviours in **L** and ω even when angular momentum is dependent on angular velocity can be attributed to the relationship between the Jacobi radius $r_{\rm J}$ and ω. The Jacobi radius is inversely proportional to the instantaneous orbital period Ω of a cluster. When the cluster is at pericenter, Ω is at it's largest point, and the Jacobi radius will decrease, making the cluster radius smaller, but ω increases to conserve angular momentum. Thus the change of ω will be canceled out by the changing radius of individual stars in the cluster, and thus the step function like evolution from the mass remains in the angular momentum, making the evolution of **L** a step function.

3.3 Evolution of Angular Momentum in Spherical Coordinates

Although considering the evolution of a star system in Cartesian coordinates can be useful, globular clusters are nearly spherical objects, and considering the evolution in spherical coordinates will help us formulate a full image of the clusters. In this section, we consider the evolution of **L** and ω in spherical coordinates. We plotted 3 plots each for L_ϕ and L_θ in figure 3.5, one plot in terms of time normalized to $t_{\rm rh,i}(t/t_{\rm rh,i})$, another in terms of time normalized to the orbital period T of a cluster(t/T), and last in terms of the percentage of mass remaining in the cluster m.

Overall, we see that both L_ϕ and L_θ decreases in every plot. We also observe the step function like behaviours in the spherical coordinate as well, most notably in E06 and E08 for both L_ϕ and L_θ.

When observing the $t/t_{\rm rh,i}$ evolution of L_ϕ(top right plot), we see that E08 evolves the slowest, followed by F025, E06, E04, E02, and F075. In general, the further away the cluster is from the galaxy, the slower it evolves because of the decreased mass loss rate, as suggested by previous

sections. However, interesting thing to note is the fact that both E08 and E06 have a larger apocenter distance than F025, yet the two clusters evolves faster than F025. This result seems to suggest that although distance plays a large role in deciding the evolution rate of L_ϕ, the closer pericenter of a cluster will still be enough to speed up the evolution of a cluster, causing E06 to evolve faster than F025.

The same cannot be said for the evolution of L_θ in terms of $t/t_{\rm rh,i}$ however(bottom right plot), as F025 evolves much slower compared to any eccentric orbits. L_θ of all eccentric orbits evolve at a similar rate until at around 10 $t/t_{\rm rh,i}$ when E02 deviated away from the other eccentric orbit simulations and starts to decrease rapidly. It's worth noting that in this plot, both circular orbits and E02 starts to decrease rapidly after a certain point in the simulation, compared to their initial behaviour.

The top middle plot in figure 3.5 plots t/T versus L_ϕ. In this plot, all simulation seem to evolve at a similar rate, suggesting that the evolution of L_ϕ is heavily dependent on the number of orbital period the cluster completes. It is worth mentioning that due to the limitation in our simulation, E08 were not able to evolve to sufficient number of orbital period like the other simulations. Thus accuracy of this result must be studied further to formulate specific conclusions.

The bottom middle plot on figure 3.5 shows t/T evolution of L_θ. Unlike the L_ϕ plot, the evolution rate differs largely between simulation. In general, lower eccentric and circular orbits tend to evolve slower compared to higher eccentric orbits. F025, F075, E02, and E04 all seem to evolve at a similar rate, while E06 and E08 evolve much quicker. Thus we infer that L_ϕ is dependent on the orbital period, while L_θ is not.

The top right plot is the evolution of L_ϕ in terms of the percentage of mass remaining in the system. We see that E08 has the slowest evolution, followed by E06, E04, and with E02 and the circular orbits evolving at around the same time with F075 evolving slightly slower than F025. We saw in figure 3.1 that E08 loses mass the slowest compared to others, thus leading to a slower evolution in L_ϕ. However, it is also worth pointing out that F075 evolves slightly slower in L_ϕ even though it's mass loss rate is faster than F025. This suggests that although mass loss has some

Figure 3.5: The following plot shows the evolution of L_ϕ (top row) and L_θ (bottom row) of each simulation. Simulations of E02, E04, E06, E08, F075, and F025 are all represented by colors blue, yellow, green, red, purple, brown respectively.

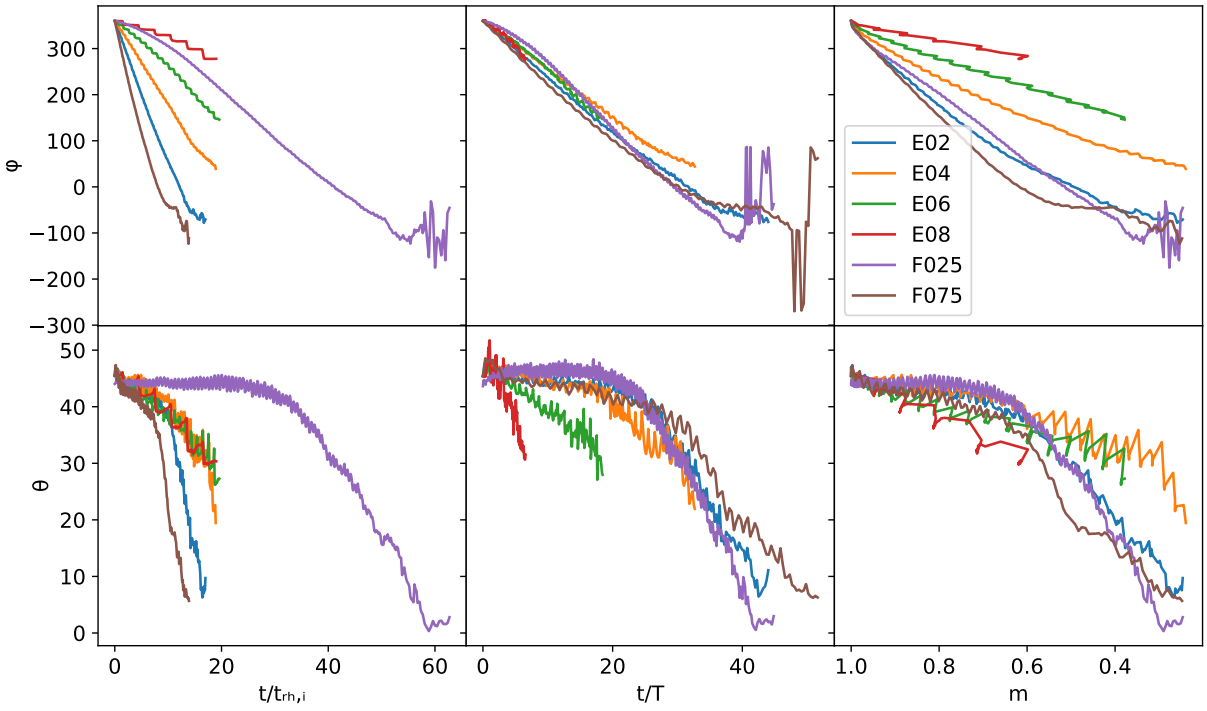

effect on L_ϕ, it is not the only factor behind it like how the orbital period T is.

The lower right plot shows the evolution of L_θ in terms of the remaining mass m in the system. We see that all simulations initially evolve at a similar rate, until E04 and E06 deviates away from the rest, starting at around 0.6 m. This suggests that L_θ is heavily dependent on the mass of the cluster and tends to decrease as less mass are present. It is worth noting that due to complication in E08 simulation, it was not able to run as long as E04 and E06. Thus it is possible that E08 also deviates away from the circular and low eccentric orbits.

3.4 Evolution of Angular Momentum in 3 Equal mass Regions

Tiongco et al. (2018) also found that, since the outer regions of the cluster tidally lock with the galaxy before the inner regions, the direction of a cluster's rotation varies with radius measured from the cluster's core. For this reason, it will be wise to study $\mathbf{L}$ and ω within different regions of the cluster defined by their radius. Specifically, we calculated the radius at which $\frac{1}{3}$ and $\frac{2}{3}$ of the mass falls at a point in time for the cluster and calculated the $\mathbf{L}$ for each region. This was due to the findings in previous sections regarding the importance of a cluster's mass in the evolution of the cluster. Schematic representation is presented in figure 3.6. The time evolution of $\mathbf{L}$ for each region is plotted in Cartesian coordinates in figure 3.7 for all eccentric orbit simulations.

In all simulations, the region with the largest magnitude of angular momentum is the outer regions(red line), while the angular momentum at the inner regions(orange line) stay approximately zero. This is likely due to the fact that even with a larger angular velocity in the inner regions, it is not enough to compensate for the small radius that the stars are orbiting in. Figure 3.8 plots the time evolution of angular velocity in Cartesian coordinate, and indeed the angular velocity of the inner regions is much larger in magnitude compared to the other two regions.

While the magnitude of $\mathbf{L}$(blue line) in figure 3.7 acts as the sum of all components, magnitude of ω(blue line) in 3.8 closely follows the outer region of the cluster, and is much smaller than the magnitude of the inner/middle regions.

Besides what was mentioned above, in both $\mathbf{L}$ and ω, the sinusoidal behaviour in the x and

Figure 3.6: A schematic representation of the set up for section 3.4 The area labeled outer region contains 34% of the mass, middle region containing 33%, while the inner region containing the remaining 33%. Note that due to the high density of stars near the core, the inner region has the smallest volume while the outer region has the largest.

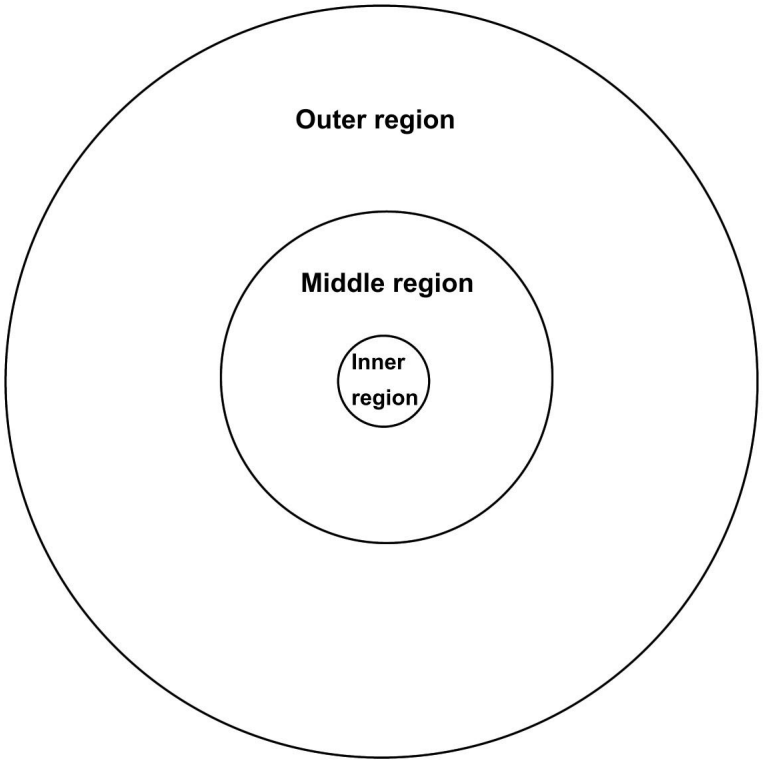

Figure 3.7: Figure showing the evolution of **L** for the eccentric orbit simulations. The inner 0-33% of the mass is denoted by the orange line, middle 34-66% by the green line, and outer 64-100% of the mass represented by the red line. The total angular momentum for the whole cluster is represented by the blue line.

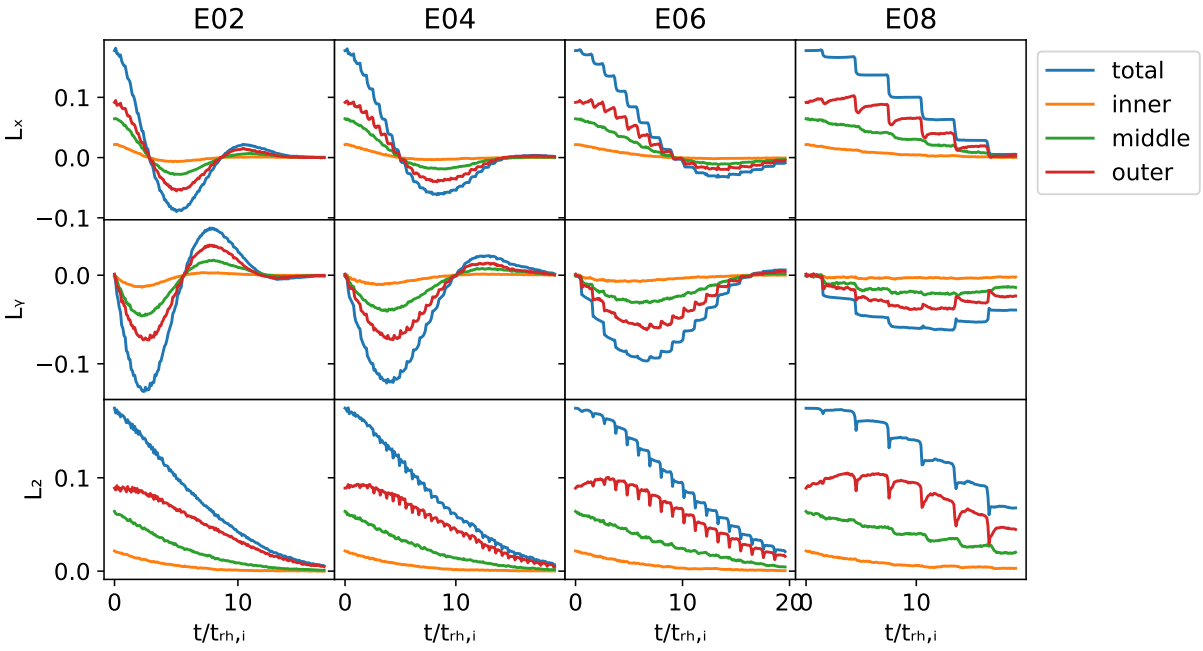

Figure 3.8: Figure showing the evolution of ω for the eccentric orbit simulations. The inner 0-33% of the mass is denoted by the orange line, middle 34-66% by the green line, and outer 64-100% of the mass represented by the red line. The total angular momentum for the whole cluster is represented by the blue line. Unlike the previous plot of $\mathbf{L}$, the inner regions have the highest angular velocity.

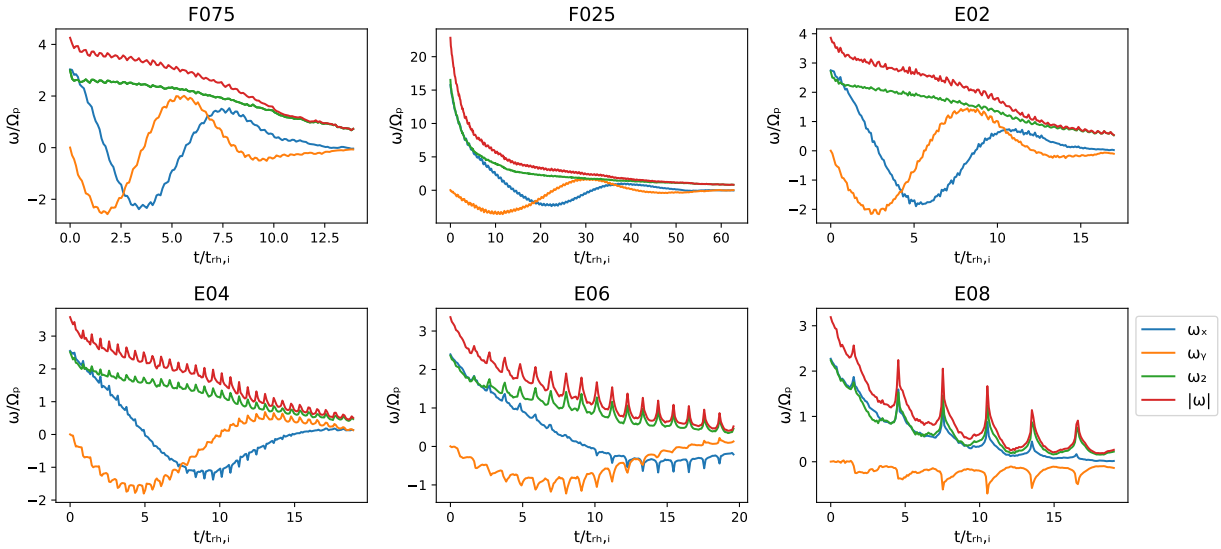

y direction seen in section 3.1 is seen here in all regions, suggesting that the cluster as a whole precesses as it evolves with time. On the other hand, the step function in $\mathbf{L}$ and the nutation in ω can only be observed in the outer regions of the cluster, likely due to the fact that the inner regions of a cluster interacts with the core of the cluster more than the host galaxy, thus the inner region is not affected as much by the host galaxy compared to the outer region.

Now we shift our attention spherical coordinates. The angular momentum in spherical coordinates for third mass region for all eccentric orbit simulations are plotted in figure 3.9. The top row shows L_ϕ, and does not change between different regions in any of the simulations. This plot suggests that L_ϕ evolves at the same rate regardless of the regions in the cluster, as long as the mass is the same across all regions. This supports the conclusion of section 3.3, where we saw that L_ϕ evolves with orbital period rather than mass, as all three regions are considered to be in the same location relative to the host galaxy.

The bottom row of figure 3.9 shows the time evolution of L_θ in each third mass region. Overall, L_θ starts out similar between each regions, then starts diverging away from each other as it evolves with time. Towards the end of the simulation, the inner regions has the largest angle of L_θ, with lowest in the outer regions. It is also worth noting that L_θ of all third mass region in E08 evolves at a similar rate. We believe this is due to the limitation in the simulation, where E08 was not able to run as long the other clusters, and thus did not have enough time for the three regions to diverge away from each other. While L_θ evolves with mass, the outer region still has the gravitational interactions with the host galaxy, which could probably be attributed to the variation between the three regions.

Figure 3.9: Figure showing the evolution of L_ϕ(top row) and L_θ(bottom row) in each third mass regions. The inner 0-33% of the mass is denoted by the orange line, middle 34-66% by the green line, and outer 64-100% of the mass represented by the red line. The total angular momentum for the whole cluster is represented by the blue line.

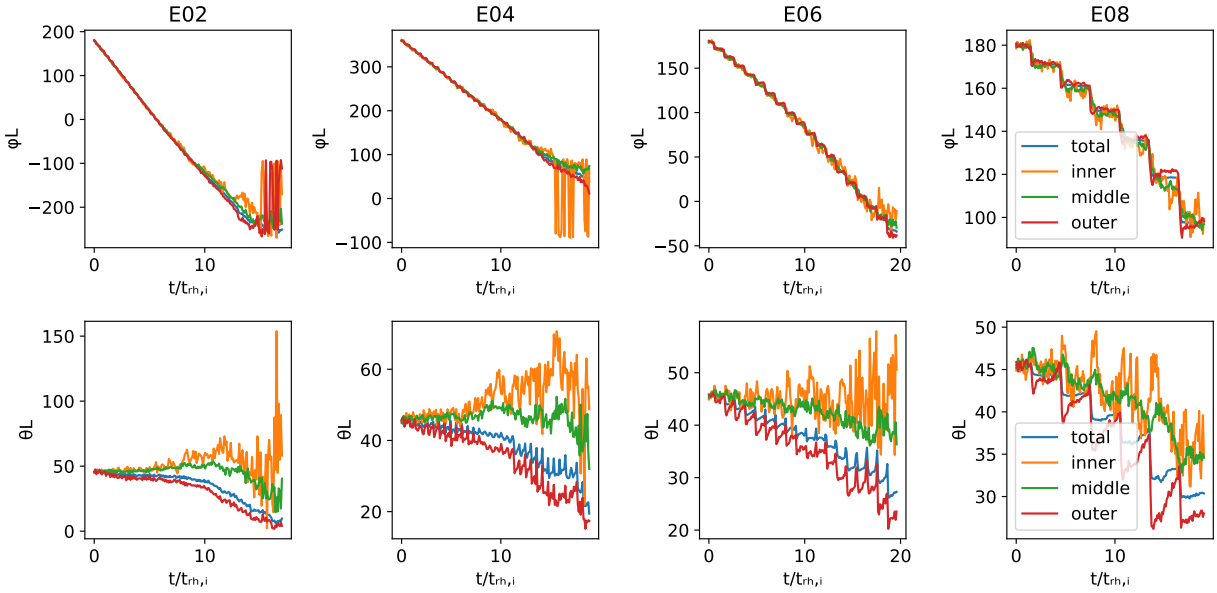

Chapter 4

Discussion

We studied the effects of different eccentricity and distance of a globular clusters relative to its host galaxy in the hopes of expanding our knowledge of their internal kinematics. As an extension, we looked at how different regions of the cluster defined by equal mass evolves differently from each other. We were able to come to the following conclusions:

- Both the angular momentum and angular velocity of a globular cluster is heavily dependent on the mass loss rate of the cluster.
- Globular clusters with high eccentric orbits show step function like behaviour in their angular momentum evolution, with the periods of the step function corresponding to their orbital period.
- Globular clusters with high eccentric orbits shows a nutation in angular velocity, which increases when the cluster approaches pericenter and decreases when reaching apocenter.
- Clusters with larger distance evolve slower compared to clusters that are closer to the host galaxy.
- The evolution of L_ϕ in the entire cluster seems to depend on the orbital period, while the evolution of L_θ seems to depend on mass.
- Step function and nutation found in the angular momentum and velocity of a cluster is most prominent in the outer regions of the cluster.

Overall, we found the eccentric orbits do indeed have an effect on the globular cluster. This is not because of the eccentric orbits themselves, but rather the effect eccentric orbits have on the mass loss rate of the cluster. A cluster's evolution is heavily dependent on how much mass is remaining in the system, and the eccentricities of the cluster's orbits dominates how much mass is ejected from the system at what time.

Careful consideration will be needed when comparing these data with observational data however. As mentioned in previous sections, limitations of this research, such as the computer program and the varying distance depending on eccentric orbits, would mean that these results may not be the best representation of real life globular clusters. Further studies will be needed to claim anything definitive.

However, our study does provide an insight into how globular cluster should act at a specific point in their life. Models like these could be used to make predictions on how a cluster will evolve in the future. Since most globular clusters in the galaxy are in eccentric orbits, it is likely that they will also show a step function like behaviour in their mass loss and angular momentum. For example, a cluster that has a slower mass loss rate could be inferred to be a high eccentric cluster at its apocenter.

Overall, we succeeded in expanding the knowledge of globular clusters, but further work will be able to give definitive answers to how they evolve kinematically.

Chapter 5

Future Works

Although we have successfully expanded our knowledge of the evolution in internal kinematics of globular cluster, there are multiple areas to improve and expand on, rather due to the limitation of our study, or other interesting behaviours we saw in this study that we did not have enough time to dive into.

Few examples of limitation in our study includes the limitation of the software used. As mentioned before, NBODY6 is a simulation program which has difficulty simulating globular clusters that experiences core collapse. Due to this reason, we were unable to expand on the effect of the orbital period on L_ϕ in section 3.3 for high eccentric orbits. In general, running longer simulations with more particles will be beneficial when comparing theoretical data with observational results.

Another limitation we faced were a lack of time to investigate the behaviours of L_θ in spherical coordinates more closely. Questions such as the cause of sudden decrease of L_θ in circular and less eccentric orbits were not answered due to time constraints. Future works considering a larger range of eccentricities and time could potentially solve these questions.

Finally, future works would consider the radial velocity profile of each cluster to see how eccentric orbits affect the evolution of velocity in different radius. An example of such exploration are shown in figure 5.1.

The figure shows the radial profile of the average velocity in different radius of the cluster normalized to r_h at specific points in their evolution for E02 simulation. We can see that the velocity in the ϕ direction seem to decrease to a specific point, before increasing back up to it's

Figure 5.1: Figure showing the radial profile of average stellar velocity in the ϕ direction of the cluster for the simulation E02.

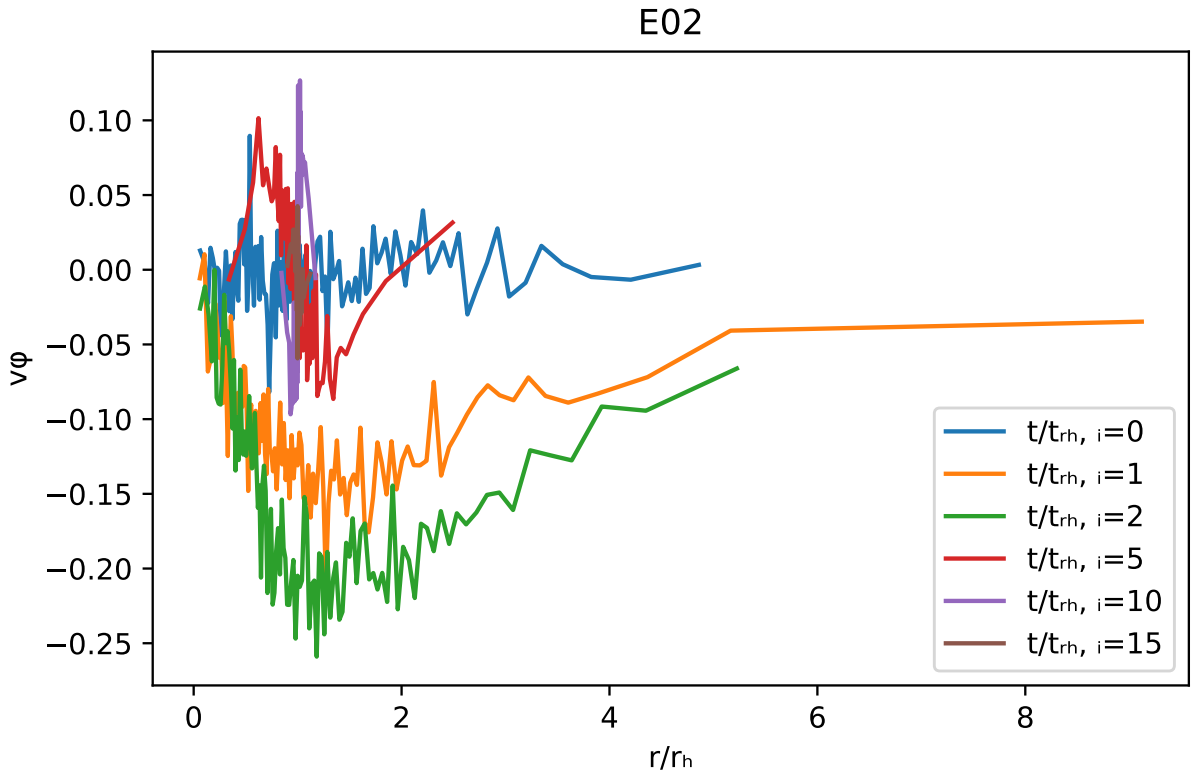

original position. Seeing whether this effect can be seen for all simulations could give us a better understanding on how radial velocity is affected by the eccentricitiy of the orbit.

Our hope is that future work will address all the issues above to expand our knowledge of globular clusters.

Bibliography

O. Anagnostou, M. Trenti, and A. Melatos. Hierarchical Formation Of An Intermediate Mass Black Hole Via Seven Mergers: Implications For GW190521. arXiv e-prints, art. arXiv:2010.06161, Oct. 2020.

N. Bar, S. Danieli, and K. Blum. Dynamical friction in globular cluster-rich ultra-diffuse galaxies: the case of NGC5846-UDG1. arXiv e-prints, art. arXiv:2202.10179, Feb. 2022.

M. H. Fabricius, E. Noyola, S. Rukdee, R. P. Saglia, R. Bender, U. Hopp, J. Thomas, M. Opitsch, and M. J. Williams. Central Rotations of Milky Way Globular Clusters. apjl, 787(2):L26, June 2014. doi: 10.1088/2041-8205/787/2/L26.

D. Heggie and P. Hut. The Gravitational Million-Body Problem: A Multidisciplinary Approach to Star Cluster Dynamics. 2003.

S. Ninkovic. On eccentricities of globular cluster galactocentric orbits. Astronomische Nachrichten, 304(6):305–311, Jan. 1983. doi: 10.1002/asna.2113040605.

K. Nitadori and S. J. Aarseth. Accelerating NBODY6 with graphics processing units. mnras, 424 (1):545–552, July 2012a. doi: 10.1111/j.1365-2966.2012.21227.x.

K. Nitadori and S. J. Aarseth. Accelerating NBODY6 with graphics processing units. mnras, 424 (1):545–552, July 2012b. doi: 10.1111/j.1365-2966.2012.21227.x.

M. A. Tiongco, E. Vesperini, and A. L. Varri. Kinematical evolution of tidally limited star clusters: rotational properties. mnras, 469(1):683–692, July 2017. doi: 10.1093/mnras/stx853.

M. A. Tiongco, E. Vesperini, and A. L. Varri. The complex kinematics of rotating star clusters in a tidal field. mnras, 475(1):L86–L90, Mar. 2018. doi: 10.1093/mnrasl/sly009.

A. L. Varri and G. Bertin. Self-consistent models of quasi-relaxed rotating stellar systems. In G. Bertin, F. de Luca, G. Lodato, R. Pozzoli, and M. Romé, editors, Plasmas in the Laboratory and the Universe: Interactions, Patterns, and Turbulence, volume 1242 of American Institute of Physics Conference Series, pages 148–155, June 2010. doi: 10.1063/1.3460118.

J. J. Webb, N. Leigh, A. Sills, W. E. Harris, and J. R. Hurley. The effect of orbital eccentricity on the dynamical evolution of star clusters. mnras, 442(2):1569–1577, Aug. 2014. doi: 10.1093/mnras/stu961.